A Discussion on Interstellar Pickup Ions

By: Brad Cannon

Senior Thesis-Spring 2013

Chapter 1: *Introduction to the Solar Wind*

Although there is a lot known about the physics that dictates the movement of the planets and starts throughout the night sky, little is known about the medium which encompasses these heavenly bodies. Let us consider our own solar system as an example of this. The reason for the orbit of planets around the Sun has been well known for quite some time. In addition to this, the predictability of these motions is represented well with the assistance of Einstein's theory of General Relativity. However, as technological advancements in science have given us the ability to send spacecraft to the farthest reaches of our solar system, scientists have come to discover that there are many physical phenomenon's that are unexplained. An example of this is the solar wind. Since the Sun is the source of this highly energetic and multifaceted medium, we must also observe and study it closely in order to better understand the medium that it produces.

The solar wind is an expanding gas composed mostly of protons and electrons moving radially away from the solar source. It expands at high speed, roughly ten times the speed of sound, to form a high Mach number flow. As the solar wind expands outward, the speed remains constant and the density decreases. Table 1 is an example of solar wind parameters consisting of velocity, density, temperatures, etc. observed at different radial distances from the Sun.

Table 1 – Example of different solar wind parameters and their values at 1 AU and beyond [1].

Measured Parameter	Typical value at 1 AU	Variation with heliocentric radius
Composition of Ion Component	~96% H^{+} ~4% He^{++}	Constant
Flow Velocity	~400 km s^{-1} Radially directed	Constant
Density	~6 protons cm^{-3}	$\propto r^{-2}$
Magnetic Field	$\sim 5 \times 10^{-5} G$ oriented in ecliptic plane at about 45° to radial direction	Radial component $\propto r^{-2}$
Proton Temperature	$\sim 4 - 10 \times 10^{4} K$	$\propto r^{-a}, \frac{2}{7} \lesssim a \leq \frac{4}{3}$
Electron Temperature	$\sim 10 - 20 \times 10^{4} K$	$\propto r^{-b}, \frac{2}{7} < b \leq \frac{4}{3}$
Helium Temperature	~4 ×proton temperature	?

There are other additional factors which complicate the radial movement of the solar wind. One of them is the magnetic field that the Sun generates, and the other is the Suns rotation. As you may or may not know, the Sun is a moderately static body with an intrinsic rotation about an axis, just like the Earth. Due to this rotation, the solar wind ejected from the Sun will travel in a radial and azimuthal fashion. In addition, the solar wind is largely comprised of charged particles. This forces the Suns magnetic field to be stretched in a spiral fashion. The theory of the solar wind spiral motion was first developed in 1958 by the space plasma physicist Eugene Parker [2][3][4]. Due to his discovery, we now refer to this behavior as the Parker spiral. Figure 1 is an example of the Parker spiral and the current sheets that are subject to its existence.

As previously stated, the expanding solar wind carries with it an extension of the Suns magnetic field. The magnetic field serves as "glue" that holds together the charged particles and facilitates their collective behaviors. The ions, in turn, provide the momentum to drive much of the physics of the solar wind. The momentum of the charged particles within the solar wind is

characterized by ram pressure. When the ram pressure equals the thermal pressure of the interstellar plasma, the flow of the solar wind stalls. This static state of the solar wind then induces a reverse shock which forces the solar wind to flow around the Sun and away from the incoming interplanetary plasma. This shock is called the termination shock. There is thought to be another shock associated with the motion of the heliosphere through the medium of space. We believe this shock exists after the termination shock and within the interstellar medium. We call this the heliospheric bow shock. Figure 2 is an example of both of the termination shock and the heliospheric shock.

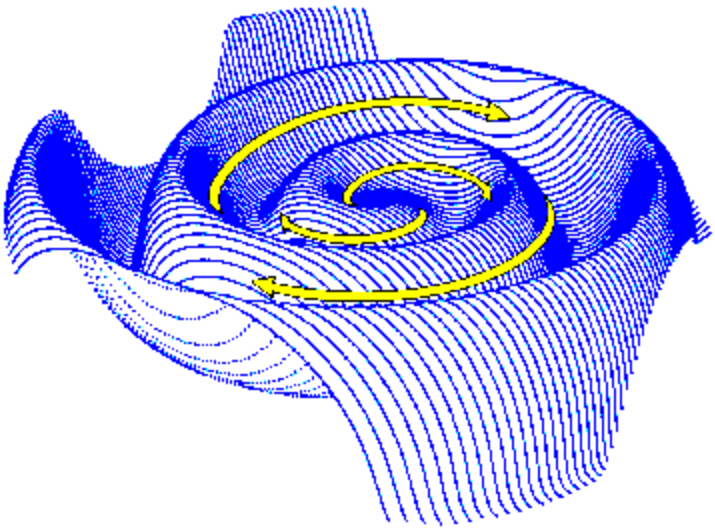

Figure 1 – Spiral structure of the interplanetary magnetic field together with heliospheric current sheets. [5]

The solar wind is a complicated system for several reasons. One of the reasons is the fact that it is often represented as a fluid. In addition to the fluidity of this medium, there is also a traversing magnetic field inside it. The magnetic field is created by the Sun and is another complicated component of the system it generates. Due to these features of the solar wind, we often describe it as being in a plasma state. A plasma is a gas of electrically charged particles that exhibits collective behavior such as supporting wave modes involving the cohesive motion of the particles.

The Sun is not the only source of deposited material in our solar system. There are also a great number of particles that enter our solar system from different parts of the universe. While the source of these particles is largely unknown, so too is the science that encompasses them

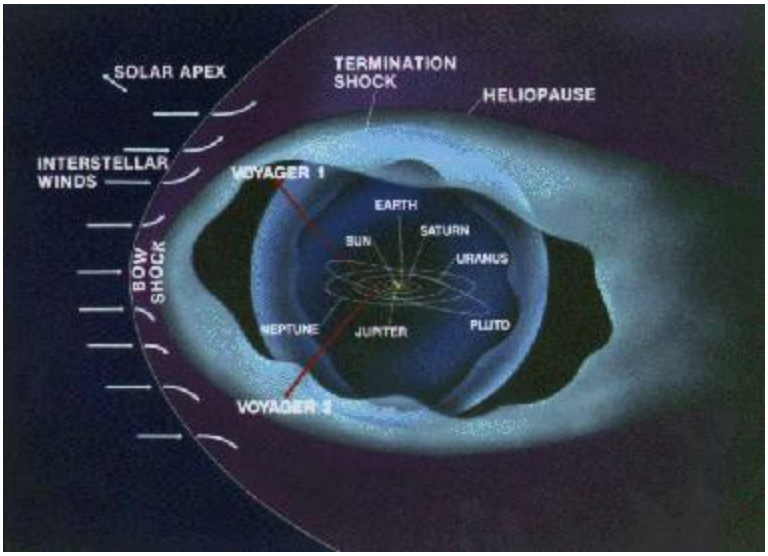

Figure 2 - Representation of the heliosphere and its interaction with the interstellar medium. The spherical shaped object surrounding our solar system is called the termination shock. The material outside of the termination shock is the heliospheric shock. [6]

once they enter our solar system. These particles can come in a variety of different masses, charges, and elements. Since the solar wind is largely composed of charged particles, many charged particles from other parts of the universe are pushed away as a consequence of Coulomb repulsion. Although this would lead many to believe that no particle can enter our solar system, some still have the ability to pass through the solar wind unperturbed. These particles are those which are neutrally charged particles. An example of a neutral particle is a neutron or any element whose electron count matches its proton count. What happens to these particles once they are inside the solar wind is the purpose and scope of this thesis. Moreover, due to the dominant abundance of the element hydrogen, the science presented in this thesis will solely concentrate on this elemental specie.

Chapter 2: *Ionization of Interstellar Neutrals*

As stated in the previous chapter, this study will only focus on the elemental specie of hydrogen. It is important to define what the phrase ‘interstellar neutral’ means in the title of this chapter. Let the phrase interstellar neutral be defined as any neutral hydrogen particle not originally released from the Sun and therefore of outer solar system origin.

To continue the story of interstellar neutrals, we must talk about what happens to them once inside the solar wind. As previously stated, the penetrating particles are neutral, whereas the solar wind is of charged nature. However, an important question must be asked about the possibility of a charged solar wind particle colliding with an interstellar neutral. This process is defined as charge exchange. Charge exchange happens when an electron of an interstellar neutral is knocked off of it or 'exchanged' with the colliding solar wind particle. Once the interstellar neutral loses its electron it then becomes ionized and therefore subject to the repulsive Coulomb force of the solar wind.

In addition to charge exchange, there is another process in which an incident neutral particle can lose its electron. This other process is known as photo ionization. Since the Sun produces a large amount of charged particles, it also produces a large amount of photons. Much like the charged solar wind particles, the particles of light also travel away from the sun in a radial fashion. Due to this, there is a chance that a traveling photon can come into contact with an interstellar neutral. If this occurs, the photon has the ability to remove the electron from the neutral, thus causing it to be ionized. A neutral hydrogen atom is subject to both charge exchange and photo ionization.

The mathematics for the number of neutral ion species as a function of radial distance to the Sun is well known [7]. The equation for neutral species goes as follows:

$$N_i = N_{io} \cdot e^{-\frac{\lambda}{r}} \quad \textbf{(1)}$$

where N_i represents the neutral ion density of a given species 'i', N_{io} is a known constant and represents the neutral density at the terminal shock for a given species 'i', λ represents another constant equal to 5.6 AU, and r represents the radial distance to the sun in astronomical units (AU). The neutral density at the terminal shock is $N_{Ho} = 0.1\ cm^{-3}$ [8][9] for hydrogen. Let it be

known that the previous constant is in units of number density. Although the terminal shock constants appear to be in units of cm^{-3}, the units should really be thought of as *number of neutral species / cm*^{3}.

Photo ionization rates and charge exchange rates for interstellar neutrals are also well known. The charge exchange rate for a given neutral species is proportional to the proton flux within the solar wind:

$$\alpha = \sigma \cdot n_{SW} \cdot V_{SW} \quad \textbf{(2)}$$

where α is the charge exchange rate for hydrogen in units of s^{-1}, σ is the cross sectional area of a proton which is $\sigma = 2.\ \times 10^{-15}\ cm^2$, n_{SW} represents the number density of protons within the solar wind as measured by the spacecraft, and V_{SW} is the solar wind velocity also measured by the spacecraft. Due to the fact that charge exchange ionization only pertains to the neutral hydrogen species, it is not necessary to include an 'i' subscript in the preceding equation. Once more, although the units of charge exchange are technically s^{-1}, the units should really be thought of as *number of hydrogen collisions / s.*

This chapter will be concluded by introducing a final equation which utilizes the previous two equations in order to predict the total number of newly ionized particles that will be 'picked up' by the solar wind. The equation goes as follows:

$$n_i = \beta_i \cdot N_i \cdot \tau_{acc} \quad \textbf{(3)}$$

where n_i is the total number of newly ionized particles, β_i represents the total ionization rate for the given particle species 'i', and τ_{acc} is a new parameter which has not yet been discussed. This parameter will be known as the accumulation time of the particles. Since the accumulation time has advanced computational and conceptual significance, it will not be thoroughly discussed in this chapter. Let it be noted that the value for the photo ionization rate is $1 \times 10^{-7}\ s^{-1}$ [10] at

one AU, and scales as r^{-2}, the radial distance of the spacecraft to the Sun. Now that the ionization process for interstellar neutrals is well known and well described, we will begin to discuss the consequences of this ionization process in the next chapter. Furthermore, we will find that this ionization process is responsible for magnetic field waves observed by the Voyager and Ulysses spacecraft, respectively.

Chapter 3: *Magnetic Waves Due to Newborn Interstellar Pickup Ions*

The Sun is responsible for the majority of material that encompasses the interstellar medium. One of the more important aspects of this medium is the Suns magnetic field which spans enormous distances in our solar system. Due to the existence of this magnetic field, any charged particle within the medium is subject to the Lorentz force law of electromagnetism which goes as $\vec{F} = q(\vec{E} + \vec{v} \times \vec{B})$. The electromagnetic force of the magnetic field causes both thermal and newly ionized particles to orbit the magnetic field in a cycloid motion. An example of this motion is depicted in Figure 3. Since the ionized particles travel in a cycloid motion, there must be a frequency which describes the motion. We call this the cyclotron frequency [11] which is defined as:

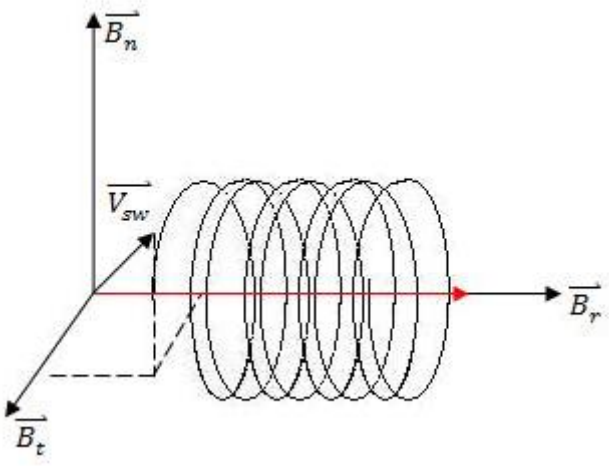

Figure 3 – Illustration of cycloid motion of newly ionized interstellar pickup ions. B_r represents the radial component of the magnetic field, B_t is the cross product of the solar rotation axis and the radial direction, and B_n is the cross product between the r and t directions, respectively. V_{sw} denotes the velocity vector of the solar wind. The red arrow represents the direction of the local magnetic field in the solar wind. Finally, the curled line represents the complicated cycloid motion of a charged particle about a magnetic field line.

$$f_i = \frac{Ze|\vec{B}|}{2\pi m_i c} \quad \textbf{(4)}$$

where f_i is the cyclotron frequency for a given species of ionized particle 'i', Z is the charge state for ionized species 'i', $e = 1.6 \times 10^{-19}$Coulombs is fundamental charge of a proton, $|\vec{B}|$ is the magnitude of the Suns magnetic field vector, m_i is the mass of the ionized particle 'i', and c is the speed of light. All of the quantities in Equation 4 above are intended to be in Gaussian cgs units.

The first affect of cycloid motion is that an ion becomes 'tied' to the magnetic field lines and therefore cannot escape. Ionized particles tied to the magnetic field give it mass and therefore inertial properties. In addition to the newly added mass, magnetic field lines also have tension. The existence of inertia and tension in the magnetic field lines facilitates the existence of low frequency waves. There are numerous texts that derive and describe the existence of low frequency magnetic waves; however, we will not focus on these derivations in this paper.

There are two types of low frequency magnetic waves found in the solar wind: 1) Alfvén waves and 2) fast mode waves. Alfvén waves are loosely analogous to waves on a string. The magnetic field provides the tension of the string and the ions provide the mass of the string. More precisely, Alfvén waves propagating parallel to the background magnetic field are circularly polarized waves that oscillate in the same sense as an ion orbits the magnetic field. Circular motion of this type is referred to as 'left hand' polarized. Alfvén waves have the dispersion relation

$$\omega = \vec{k} \cdot \overrightarrow{V_a} \quad \textbf{(5)}$$

where ω represents the frequency of the Alfvén wave, $\vec{k}$ is the wave number of the Alfvén wave, and $\overrightarrow{V_a}$ is the Alfvén velocity. The Alfvén velocity has its own equation which goes as

$$\overrightarrow{V_a} = \frac{\overrightarrow{B_o}}{\sqrt{4\pi\rho}} \quad \textbf{(6)}$$

where $\overrightarrow{B_o}$ is the average magnetic field vector and ρ is the mass density of the solar wind. We can describe the Alfvén wave as

$$\vec{B}(\vec{x}, t) = \delta\vec{B} \cdot e^{i(\vec{k}\cdot\vec{x} - \omega t)} \quad \textbf{(7)}$$

where $\delta\vec{B}$ is the amplitude of the transverse fluctuation of the magnetic wave. If we apply Maxwell's equation $\nabla \cdot \vec{B} = 0$ to Equation 7, we find that

$$\delta\vec{B} \cdot \vec{k} = 0 \quad \textbf{(8)}$$

This shows that Alfvén magnetic fluctuations are perpendicular to the propagation direction of the magnetic waves.

The other low frequency wave mode that can be observed in the solar wind is the fast mode wave. Fast mode waves are 'right hand' polarized waves. The dispersion relation for a fast mode wave is

$$\omega = kV_a \quad \textbf{(9)}$$

For fast mode waves, $\delta\vec{B}$ is still perpendicular to *k*, but since *k* is not perpendicular to the background magnetic field, $\delta\vec{B}$ can have a projection onto the background magnetic field, $\overrightarrow{B_o}$. Why the fast mode wave dispersion relation does not have a dot product and why they are oppositely polarized from Alfvén waves is beyond the scope of this paper.

Most of the theories for pickup ions have concentrated on the component of the wave number *k* that is parallel to the background magnetic field. The principle difference between Alfvén waves and fast mode waves is their polarization. Both waves travel at the Alfvén speed, and the Alfvén speed is typically one tenth of the solar wind speed. A thermal ion and an Alfvén wave have the same polarization, whereas thermal ions and fast mode waves do not. This applies

to the situation where the wave propagates over the thermal ion. If an energetic particle moves through the solar wind at the solar wind speed, wave propagation becomes largely irrelevant. A particle senses not the polarization of the waves, but the spatial structure of the waves. When the motion of an energetic particle matches the spatial structure of the magnetic wave, they are said to be in resonance. For this reason, energetic particles resonate with sunward propagating fast mode waves rather than Alfvén waves.

Chapter 4: *Search for Magnetic Waves Due to Newborn Interstellar Pickup Ions*

A magnetometer with high resolution will record magnetic field measurements every one to three seconds; whereas a magnetometer with low resolution will take measurements every two or three minutes. Due to the nature of interstellar pickup ions and the magnetic waves they produce, it is important to have a magnetometer with high resolution. Before we continue with our discussion of magnetic waves due to interstellar pickup ions, we must first define three important parameters associated with theses waves. The three parameters are ellipticity, percent polarization, and angle of propagation direction to the field.

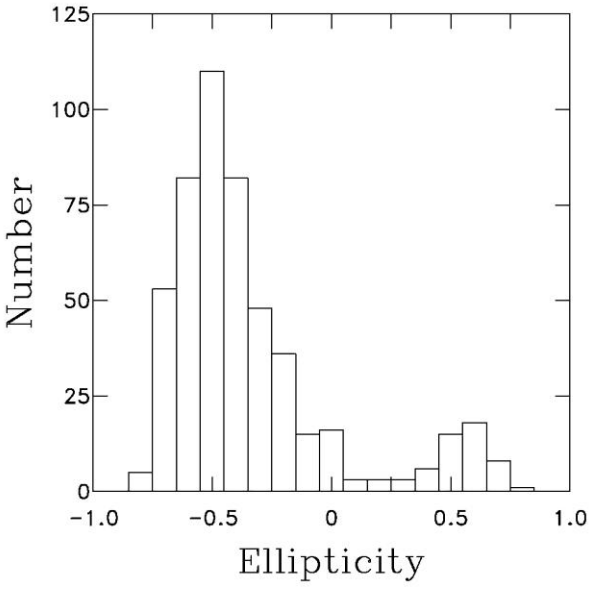

Figure 4 – A distribution of different ellipticity values for pick up ion events. The horizontal components of the bars have a rage of ±0.05. The vertical components of the bars is a count of pickup ion events that fall into one of the ellipticity ranges. [12]

Ellipticity can be defined by using three parameters of a magnetic wave. The three parameters are the major axis, the minor axis, and the direction of rotation. Since many of these waves are not perfectly circular and sometimes

two dimensional, this is an important aspect of the waves. We define positive ellipticity to be a 'right handed', or clockwise, and negative ellipticity to be 'left handed', or counterclockwise. We also define the value of ellipticity by taking the ratio of the minor axis over the major axis. Therefore, ellipticity values will have a range from -1 to +1. Figure 4 is an example of ellipticity distributions for a given set of pickup ion events [12].

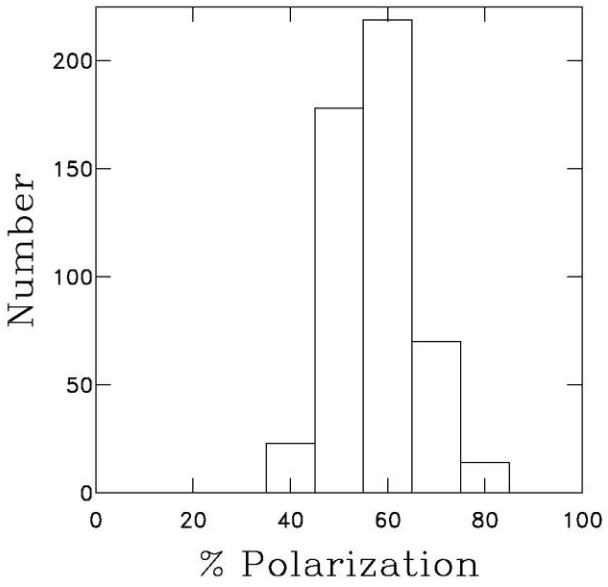

Figure 5 – A distribution of different percent polarization values for pick up ion events. The horizontal components of the bars have a rage of ±5 percent polarization. The vertical component of the bars is a count of pickup ion events that fall into one of the percent polarization ranges. [12]

Percent polarization is another important parameter for pickup ion events. Percent polarization is the quantitative measure of how 'smooth' the wave signal is. For example, if the magnetic wave signal resembled that of a stretched spring, the signal would be considered to have a high percent polarization. Conversely, if the magnetic wave signal had a general cycloid like geometry with a lot of perturbations and noise associated with it, the signal would be considered to have a low percent polarization. Figure 5 is a schematic of a percent polarization distribution for a given set of interstellar pickup ion events [12].

Finally, there is the angle of propagation direction to the field. This parameter describes the geometric angle between the direction of the solar wind flow with respect to the local magnetic field. Since the solar wind typically flows away from the Sun in the radial direction, this angle is generally just the magnetic field direction with respect to the radial direction. We

represent this parameter with the Greek character theta, and the equation for the angle of propagation direction to the field is given by:

$$\theta = \tan^{-1}\left(\frac{\sqrt{{B_t}^2+{B_n}^2}}{|B_r|}\right) \quad \textbf{(10)}$$

where B_r, B_t, and B_n represent the components of the magnetic field as mentioned in Figure 3 above. Figure 6 is an example of theta values versus heliographic distance for a given set of pickup ion events [12].

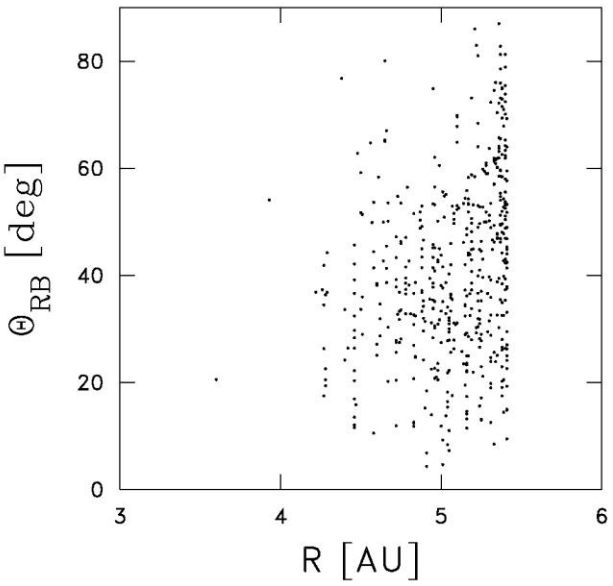

Figure 6 – Plot of angle of propagation direction to the field (Θ_{RB}) versus heliographic distance (R) measured in astronomical units. One AU is defined as the distance from the earth to the sun and is roughly equal to 1.5×10^8 km. As you can see, the existence of a pickup ion event is not dictated by the Θ_{RB} value. [12]

Now that we have defined all of the preceding terms, it is appropriate to discuss how they are applied to high resolution data. Once high resolution data is collected, we then use Fourier transforms so that we can view the results in frequency space as a function of spacecraft time. Spacecraft time can be defined as the time in which the data was taken in terms of Earth time, or universal time. We then use the mathematical equations above to obtain results for ellipticity, percent polarization, and the angle of propagation direction to the field. This allows us to take a given set of data and search for characteristics associated with interstellar pickup ion events as a function of spacecraft time. An example of this is illustrated below in Figure 7.

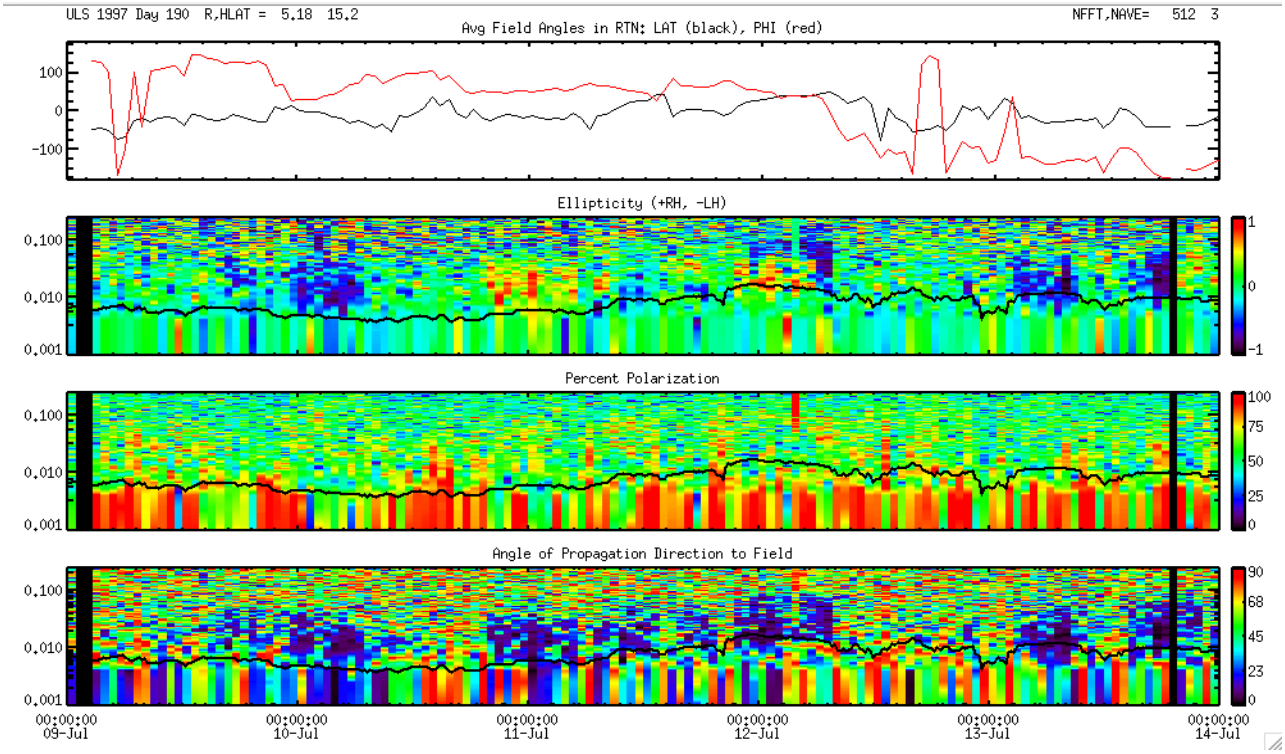

Figure 7 – An example of a color spectagram for ellipticity, percent polarization, and angle of propagation direction to the field. This data was taken by the Ulysses spacecraft from 07-09-1997 to 07-14-1997. Clear elliptical signatures and propagation angle signatures pertaining to pickup ion events can be seen near 10-Jul, 12-Jul, and 13-Jul.

Once we believe that a pickup ion event has been found from the color spectagram, we then use the spacecraft times to do a more in depth analysis of the high resolution magnetic field data. By obtaining the spacecraft start and stop times for potential pickup ion events, we can then create a power spectrum to see whether or not an event actually took place in that time span.

Contained within each power spectrum for potential events are four figures: 1) Power: B Transverse, B Parallel, 2) Angle of Propagation to Field, 3) Percent Polarization, and 4) Ellipticity. The transverse and parallel power spectrum allows us to determine the amount of power that a particular pick up ion event has created as a function of frequency. Although we can already observe the angle of propagation to the field, percent polarization, and ellipticity from the color spectagram, it is important to view them using power spectra in order to more

accurately determine their values. Examples of two different power spectra's are depicted below in Figure 8 and Figure 9.

As discussed in the captions, Figure 8 is confirmed to be a pickup ion event; whereas, Figure 9 is confirmed to not be a pickup ion event. This feature is very confusing seeing that Figure 9 contains a good ellipticity signature as well as a good angle of propagation to the field signature. The reason for the existence of a pickup ion event in a given region of space will be the subject of the next chapter. In addition, we will also discuss why we see pickup ion events at certain spacecraft times, and why we do not see pickup ion events at certain spacecraft times.

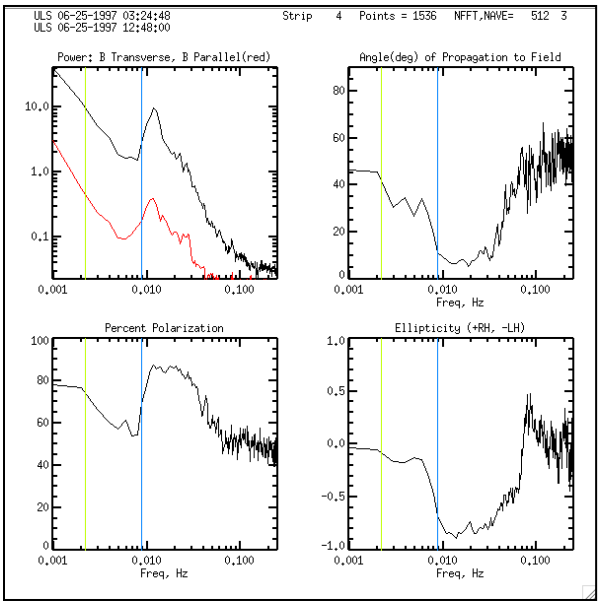

Figure 8 – An example of a power spectrum as observed by Ulysses spacecraft. Notice that in the upper left box there is a clear power enhancement above the background. This allows us to determine that this is a pickup ion event.

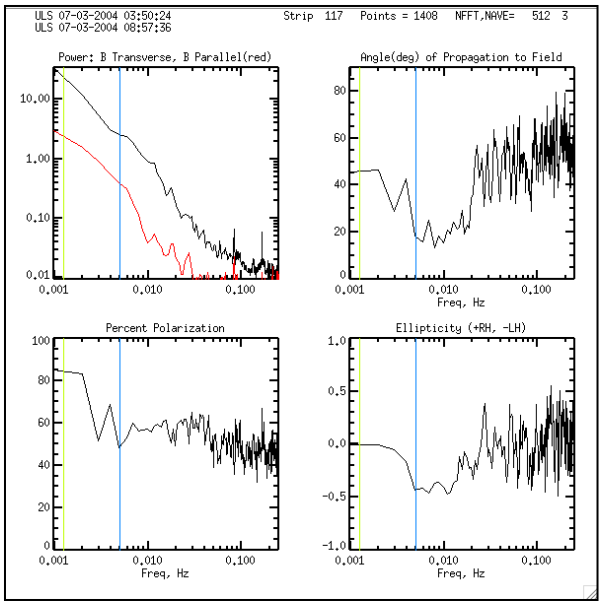

Figure 9 – An example of a power spectrum as observed by Ulysses spacecraft. Notice that in the upper left box there is no clear power enhancement above the background. This allows us to determine that this is not a pickup ion event.

Chapter 5: *Accumulation and Destruction Rates*

With every possible pickup ion event there is an associated accumulation rate and destruction rate. An accumulation rate is defined as the amount of energy that newly ionized interstellar pickup ions inject into the Suns magnetic field to create waves. The accumulation rate has units of energy per unit time. The destruction rate can be defined as how rapidly the energy from newly ionized interstellar pickup ions is dissipated into the background. This effect is often referred to as the 'turbulent cascade', and is also in units of energy per unit time. An example of the turbulent cascade is when a cigarette is lit in a small room that contains a uniform, steady state gas. When the cigarette is lit, it emits smoke which is initially ejected in an organized manner. Moreover, if one looks closely, the smoke appears to eject in spiral-like structures resembling a hurricane. Over time these spiral-like structures, or 'eddy's', break up into smaller and smaller sized eddy's. Eventually, the eddy's will reach a scale that is unobservable, and therefore is represented as background.

The turbulent cascade was first studied and mathematically described by Kolmogorov in 1941. Although there are many other theories in space physics that attempt to describe the nonlinear behavior of energy dissipation, we choose to use Kolmogorov's theory. He describes the nonlinear destruction rate as [13]:

$$\varepsilon = \frac{f^{5/2} \cdot E(f)^{3/2} \cdot 21.3^3}{V_{sw} \cdot N^{3/2}} \quad \textbf{(11)}$$

Where ε is the destruction rate, f is the cyclotron frequency, E(f) is the power observed at the cyclotron frequency, V_{sw} is the velocity of the solar wind, and N is the density of protons in the local solar wind environment.

In order to explain how the accumulation rate is obtained, we must first discuss the theory of Lee and Ip [14]. Lee and Ip were the first to provide a mathematical formulation for pickup ion events. In their paper, they provide an equation which attempts to predict the power spectrum that a pickup ion will create given a particular set of parameters. The equation goes as:

$$I_{\pm}(k,\infty) = \frac{1}{2}\left[\sqrt{C(k)^2 + 4I_{+}(k,0)I_{-}(k,0)} \pm C(k)\right] \quad \textbf{(12)}$$

and $C(k)$ is defined as:

$$C(k) \equiv I_{+}(k,0) - I_{-}(k,0) + 2\pi N V_A m|\Omega|k^{-2}\left[\Omega k^{-1} v_o^{-1} - \frac{(\Omega k^{-1} v_o^{-1} - \mu_o)}{|\Omega k^{-1} v_o^{-1} - \mu_o|}\right] \quad \textbf{(13)}$$

$$k = \frac{2\pi f}{v_o} \quad \textbf{(14)}$$

where N is the number of ionized particles, V_A is the Alfvén speed, m is the mass of a proton, Ω is the cyclotron frequency multiplied by 2π, k is the wave number associated by the cyclotron frequency, v_o is the solar wind speed, and μ_o is defined as the $\cos(\Theta)$. In addition, Equation 12 and Equation 13 both contain another parameter, I. I is the predicted power for a given wave number k, and for an amount of time t. In addition, I also has + and – subscripts in Equation 12 and Equation 13. The + subscript describes anti-sunward propagating waves, while the – subscript describes sunward propagating waves. The reason for this is the nature of the r-t-n coordinate system that we use; such that, the radial direction is defined as positive when going away from the center of the Sun. In Equation 12 and Equation 13, $I_{+}(k,0)$ and $I_{-}(k,0)$ represent the observed background power level for an anti-sunward and sunward propagating wave at a given wave number k, respectively. Finally, $I_{\pm}(k,\infty)$ represents the power level of a wave number k for all time.

Since we do not know the number of ionized particles, Equation 12 and Equation 13 are no good if we want to predict power spectra for pickup ion events. Therefore, we use Equation 3

in place of the variable N in Equation 13. From Ulysses observations, we already know the Alfvén speed, cyclotron frequency, solar wind velocity, and angle of propagation to the field. This means that the only unknown parameter in Equation 12 is the accumulation time (τ_{acc}). Using computer programming, we can plot the predicted wave power as a function of accumulation time. The result of this plot is a straight line. By obtaining the slope of this line, we have acquired a number which is in units of energy per unit time. We define this number as the accumulation rate (dE_W/dt).

With every potential interstellar pickup ion event, there is an associated accumulation rate and destruction rate. From the literature above, we can obtain these rates by both using the observations of our spacecraft, as well as using computer programming techniques. In addition, we can also obtain an accumulation rate and a destruction rate for any non pickup ion event. Once we have obtained these rates for event and non event regions, we choose to plot them against each other [15].

Figure 10 is a plot of the destruction rate versus the accumulation rate. The black circles in the plot represent non event regions and the red triangles represent pick up ion events. Also located on the graph is a dashed line. This line represents locations where the destruction rate is equal to the accumulation rate. As you can see from the graph, the events and non events are clearly separated at the dashed line boundary. This suggests that pick up ion events

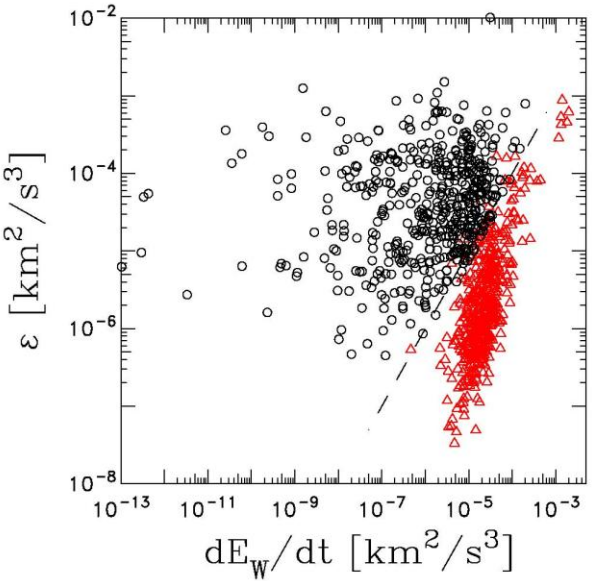

Figure 10 – Plot of destruction rate (ε) versus accumulation rate (dE_W/dt). The black circles represent non events and the red triangles represent pick up ion events. The dashed line separating the two groups is a one-to-one comparison ($\varepsilon = dE_W/dt$). [15]

only exist when the accumulation rate is greater than the destruction rate. Conversely, non event regions are those where the destruction rate is greater than the accumulation rate. Due to the clear separation of events from non events, we have now answered the question of why we see pickup ion events in certain regions and why we do not see pick up ion events in other regions.

Chapter 6: *Future Interstellar Pickup Ion Research*

Although the important question of why pickup ion events happen has been answered, there are still other questions that have not been addressed. For example, in Figure 10 we showed that the great majority of pickup ion events and non events demonstrate energy conservation. However, if one looks closely at the graph it is evident that approximately ten percent of event and non events do now follow this argument. Further researching the precision of accumulation and destruction rates is necessary for pickup ion events as well as other solar wind features.

In addition, Figure 9 is a depiction of what we would consider to be a non pickup ion event. However, as previously stated, there are clear elliptical signatures in the graph which suggests the presence of waves with geometry. Since the depiction also shows no power enhancement at or near the cyclotron frequency, only one conclusion can be drawn from this observation. Clearly the background magnetic field within the solar wind can have some type of geometry associated with it. This observation is a very important one seeing that most turbulence theories, including Kolmogorov's, suggest that background magnetic fields cannot have geometric wave properties. If we want to truly understand the complicated nature of nonlinear wave destruction we must first investigate its geometric capabilities.

Finally, there exists the issue of right handed and left handed wave modes. According to our understanding of pickup ions, only left handed wave modes should be possible. However, we observe approximately five to ten percent of our wave events to be right handed as observed in Figure 4. Although many believe these enhancements are simply Alfvén waves, the issue is that the amplitudes of the waves create enhancements rivaling those of fast mode waves.

References

[1] Barnes, A., Hydromagnetic waves and turbulence in the solar wind, *Solar System Plasma Physics*, vol. 1, edited by E.N. Parker, C.F. Kennel, and L.J. Lanzerotti, pp. 249--319, North-Holland, New York, 1979.

[2] Parker, E.N., Dynamics of the interplanetary gas and magnetic fields, *Astrophys. J., 128*, 664--676, 1958.

[3] Parker, E.N., The interplanetary gas and magnetic field, *Science in Space*, edited by L. V. Berkner and H. Odishaw, McGraw-Hill, New York, 1961.

[4] Parker, E.N., Interplanetary Dynamical Processes, Wiley-Interscience, New York, 1963.

[5] Figure 1, Source Unknown

[6] Figure 2 , Source Unknown

[7] Joyce, C.J., C.W. Smith, P.A. Isenberg, N. Murphy, and N.A. Schwadron, Excitation of Low-Frequency Waves in the Solar Wind by Newborn Interstellar Pickup Ions H+ and He+ as Seen by Voyager at 4.5 AU, *Astrophys. J., 724*, 1256--1261, 2010.

[8] Gloeckler, G., Fisk, L. A., & Geiss, J. 1997, *Nature*, 386, 374

[9] Bzowski, M., M¨obius, E., Tarnopolski, S., Izmodenov, V., & Gloeckler, G., 2009, *Space Sci. Rev.*, 143, 177

[10] Ruci´nski, D., Cummings, A. C., Gloeckler, G., Lazarus, A. J., M¨obius, E., & Witte, M. 1996, *Space Sci. Rev*, 78, 73

[11] Huba, J.D., NRL Plasma Formulary, *Naval Research Laboratory*, Beam Physics Branch, Plasma Physics Division, Washington, DC, 20375-5320

[12] Cannon, B.E., C.W. Smith, P.A. Isenberg, B. J. Vasquez, N. Murphy, R. G. Nuno, A Survey of Magnetic Wave Observations in the Ulysses Data Arising from Newborn Interstellar Pickup Protons, *Journal of Geophysical Research*, 2013.

[13] Kolmogorov, A.N., The local structure of turbulence in incompressible viscous fluid for very large Reynolds numbers, *Dokl. Akad. Nauk SSSR, 30*, 301--305, 1941. *Reprinted in Proc. R. Soc. London A, 434*, 9--13, 1991.

[14] Lee, M. A., & Ip, W.-H. 1987, *J. Geophys. Res.*, 92, 11,041

[15] Cannon, B.E., C.W. Smith, P.A. Isenberg, B. J. Vasquez, C.J. Joyce, N. Murphy, R. G. Nuno, Ulysses Observations of Magnetic Waves due to Newborn Interstellar Pickup Ions and Why They are So Seldom Seen, *Astrophys. J.*, 2013.